Food & Function

PAPER

View Article Online
View Journal

Cite this: DOI: 10.1039/c8fo01614c

One-step assembly of zein/caseinate/alginate nanoparticles for encapsulation and improved bioaccessibility of propolis†

Hao Zhang,[a] Yuying Fu, *[a,b] Yujuan Xu,[c] Fuge Niu,[a] Zeya Li,[a] Chujie Ba,[a] Bing Jin,[a] Guowen Chen[a] and Xiaomeng Li[a]

The design of zein-based nanoparticles to encapsulate bioactive molecules has gained great attention in recent years. However, the use of ethanol to dissolve zein presents flammability concerns and the scale-up production of zein-based nanoparticles is also a concern. In our study, propolis loaded zein/caseinate/alginate nanoparticles were fabricated using a facile one-step procedure: a well-blended solution was prepared containing deprotonated propolis, soluble zein, dissociated sodium caseinate micelles (NaCas) and alginate at alkaline pH, and then this alkaline solution was added to 0.1 M citrate buffer (pH 3.8) to fabricate composite nanoparticles without using organic solvents and sophisticated equipment. During acidification, the alginate molecules adsorbed on the zein/NaCas surfaces by electrostatic complexation, which improved the stability towards aggregation of zein/NaCas nanoparticles under gastrointestinal (GI) or acidic pH. The nanoparticles prepared under the optimized method (method 3 sample) were of spherical morphology with a particle size around 208 nm and a negative zeta potential around −27 mV. The encapsulation efficiency (EE) and loading capacity (LC) of propolis reached 86.5% and 59.6 μg mg^{-1} by zein/NaCas/alginate nanoparticles, respectively. These nanoparticles were shown to be stable towards aggregation over a wide range of pH values (2–8) and salt concentrations (0–300 mM NaCl). Compared to free propolis, the bioaccessibility of propolis encapsulated with nanoparticles was increased to 80%. Our results showed a promising clean and scalability strategy to encapsulate hydrophobic nutraceuticals for applications in foods, supplements, and pharmaceuticals.

Received 12th August 2018,
Accepted 22nd December 2018

DOI: 10.1039/c8fo01614c

rsc.li/food-function

1. Introduction

Zein is one of the few alcohol-soluble biopolymers that has more than 50% hydrophobic amino acids.[1] As a highly hydrophobic protein, zein has a unique brick-like shape in an aqueous environment, thus, overcoming the disadvantage of hydrophilic protein-based vehicles that may require the inclusion of additional steps like cross-linking and hydrophobic modifications to harden the nanoparticles for controlled drug release.[2] Thanks to zein's promising properties of biodegradability, biocompatibility, and slower digestibility, many lipophilic compounds have been sparked to be encapsulated into zein nanoparticles. For example, β-carotene,[3,4] curcumin,[5,6] and quercetagetin[7] have been successfully encapsulated into zein–polysaccharide composite nanoparticles.

Traditional methods to fabricate zein nanoparticles usually take advantage of the solubility of zein in 55–95% (v/v) alcohol solutions or other organic solvents.[8] Specifically, due to the inherent non-polar nature of its 50% amino acid sequence, zein can be assembled into nanoparticles by simply mixing a non-solvent with the primary solvent (aqueous ethanol or other organic solvents) with dissolved zein; the process is commonly known as the anti-solvent precipitation method.[9] However, the use of ethanol and other organic solvents presents a flammability hazard in industrial production and is also not preferred in health foods.[10] Although the organic solvents can be removed by rotary evaporation, this protocol adds complexity and additional costs.[11] Thus, methods by which food nutrients can be encapsulated in the zein nanoparticles without using an organic solvent while maintaining the stability of zein in aqueous systems are the major challenges. It is worth noting that zein is soluble at high alkaline pH from 11.3 to 12.7.[11] Recently, a pH-driven method has been reported to

[a]School of Food Science and Biotechnology, Zhejiang Gongshang University, Hangzhou, 310018, China. E-mail: webfu@126.com
[b]Hangzhou College of Commerce, Zhejiang Gongshang University, Hangzhou, 311508, China
[c]College of Food Science and Technology, Nanjing Agricultural University, Nanjing 210095, China

†Electronic supplementary information (ESI) available. See DOI: 10.1039/c8fo01614c

prepare zein–sodium caseinate (NaCas) nanoparticles based on pH transition (pH ≥ 11.5 to neutral conditions) to disassemble and reassemble the protein molecules without using organic solvents and specialized equipment.[2,11,12] Briefly, the reversible assembly can be described as follows: zein is solubilized and NaCas micelles are dissociated at sufficiently high pH, and the structural interactions between zein and NaCas can be enabled by inter-chain hydrogen bonds. During neutralization, reassociation of interior structures may turn the protein complexes into co-assembled zein/NaCas nanoparticles.[13] Although this is a promising method for fabricating zein nanoparticles as delivery vehicles, the zein/NaCas nanoparticles thus formed still have some drawbacks, such as the poor aggregation stability under gastrointestinal (GI) conditions or certain pH ranges (near the NaCas isoelectric pH). The method is time-consuming since it needs titration from high alkaline pH to neutral pH using HCl, which limits their applications as oral delivery vehicles while the scalability of the pH-driven method is a concern as well. In order to improve the stability of nanoparticles, coating the outer surface of the zein/NaCas nanoparticles with the polysaccharide to modulate the electrostatic and steric repulsion between the particles is a green and simple approach. For example, alginates are water-soluble anionic polysaccharides which have been used as a good wall material for drug and bioactive food component encapsulation.[14,15] Alginate is a promising polysaccharide to fabricate oral delivery nanoparticles, which can shrink and convert into so-called insoluble alginic acid skin to protect nanoparticles from enzymic digestion.[16] Recently, partial alkaline hydrolysis of propylene glycol alginate has been used to reduce pH from 12.5 to 7.5, providing an interesting perspective in preparing zein-based nanoparticles without the tedious process of titrating the sample using HCl.[17] More effort should be made to provide another acidification strategy to scale up the pH-cycle method.

In addition, some polyphenols and essential oils can be encapsulated in different delivery systems using the pH-driven method as previous studies reported.[2,18–21] Propolis contains numerous natural polyphenols with many potentially beneficial health properties such as antioxidant, antimicrobial, and antitumor activities.[22–24] However, the application of propolis in pharmaceuticals and food products is still challenging due to its undesirable sensorial characteristics, poor water solubility, and limited bioaccessibility.[25] It is inspired whether this pH-driven method can be used to encapsulate propolis using zein, NaCas, and alginate as building blocks. How the nanoparticles influence the bioaccessibility of propolis is a question. Furthermore, it is worth investigating since propolis containing hydroxyl groups become deprotonated at alkaline pH, and this results in a negative charge that increases the water solubility. Therefore, propolis can be encapsulated into the zein/NaCas/alginate nanoparticles by mixing a well-blended alkaline solution of propolis, zein, NaCas, and alginate with citrate buffer solution. When mixing the two solutions, the pH is reduced that leads to the insolubility of zein. Meanwhile, reassociation of NaCas micelles may cause the assembling of zein with NaCas and electrostatic complexation to occur between anionic alginate molecules and cationic zein/NaCas nanoparticles. On the other hand, propolis becomes more hydrophobic and is *in situ* encapsulated in zein/NaCas/alginate nanoparticles during acidification back to acidic pH.

To verify the above hypothesis, zein/NaCas/alginate nanoparticles were first fabricated to encapsulate propolis using the pH-driven method. The effects of three diverse encapsulating approaches on the morphology of nanoparticles, the particulate characteristics and the encapsulation efficiency of propolis were examined. Furthermore, the encapsulation mechanism was investigated by Fourier transform infrared (FTIR) spectroscopy. Physical stability of nanoparticles against pH and ionic strength, *in vitro* release profile under the simulation gastrointestinal conditions and bioaccessibility were also evaluated. The results of this study can be applied to other hydrophobic nutraceuticals containing hydroxyl groups, such as curcumin, rutin and thymol.

2. Materials and methods

2.1. Materials

Zein (Lot C10079965) and sodium alginate (Lot M28618017) were obtained from Macklin Reagent Co. Ltd (Shanghai, China). Propolis was obtained from Bee Words Industry Co. Ltd, Zhejiang Province, China. NaCas from bovine milk, pepsin, pancreatin, bile extract and 2,2′-azinobis (3-ethylbenzothiazoline-6-sulfonic acid) (ABTS) were purchased from Sigma-Aldrich Corp. (St. Louis, MO, USA). Citric acid, sodium citrate, sodium hydroxide and other reagents were all of analytical grade.

2.2. Preparation of propolis loaded zein/NaCas/alginate nanoparticles

Propolis nanoparticles were prepared using three different methods in this section, and the detailed information of the procedures is shown in Fig. 1A. In Method 1, the zein/NaCas/alginate nanoparticles were prepared using a previous method with a minor modification.[14] Zein (1%, w/v) was dissolved in 80% (v/v) aqueous-ethanol solution. Sodium alginate powder and NaCas powder were dissolved in double distilled water and stirred overnight to prepare the polysaccharide (1%, w/v) and protein (1%, w/v) stock solutions, respectively. Briefly, 1.0 mL of zein solution (1%, w/v) with dissolved propolis (5 mg) was quickly poured into 9.0 mL of diluted NaCas solution under constant stirring (1000 rpm) using a syringe to obtain the zein/NaCas solution at a mass ratio of 1 : 1. The resulting mixture was stirred at 1500 rpm for 30 min and poured into 15.0 ml of diluted sodium alginate solution to obtain mixtures with a mass ratio of 1 : 1 : 1 of zein/NaCas/alginate. The pH of the mixtures was then adjusted to 4.0 using 3 M citric acid with stirring at 1500 rpm for 30 min. A rotating evaporator was used to remove ethanol (40 °C, −0.1 MPa) to obtain zein/NaCas/alginate aqueous dispersions. Double dis-

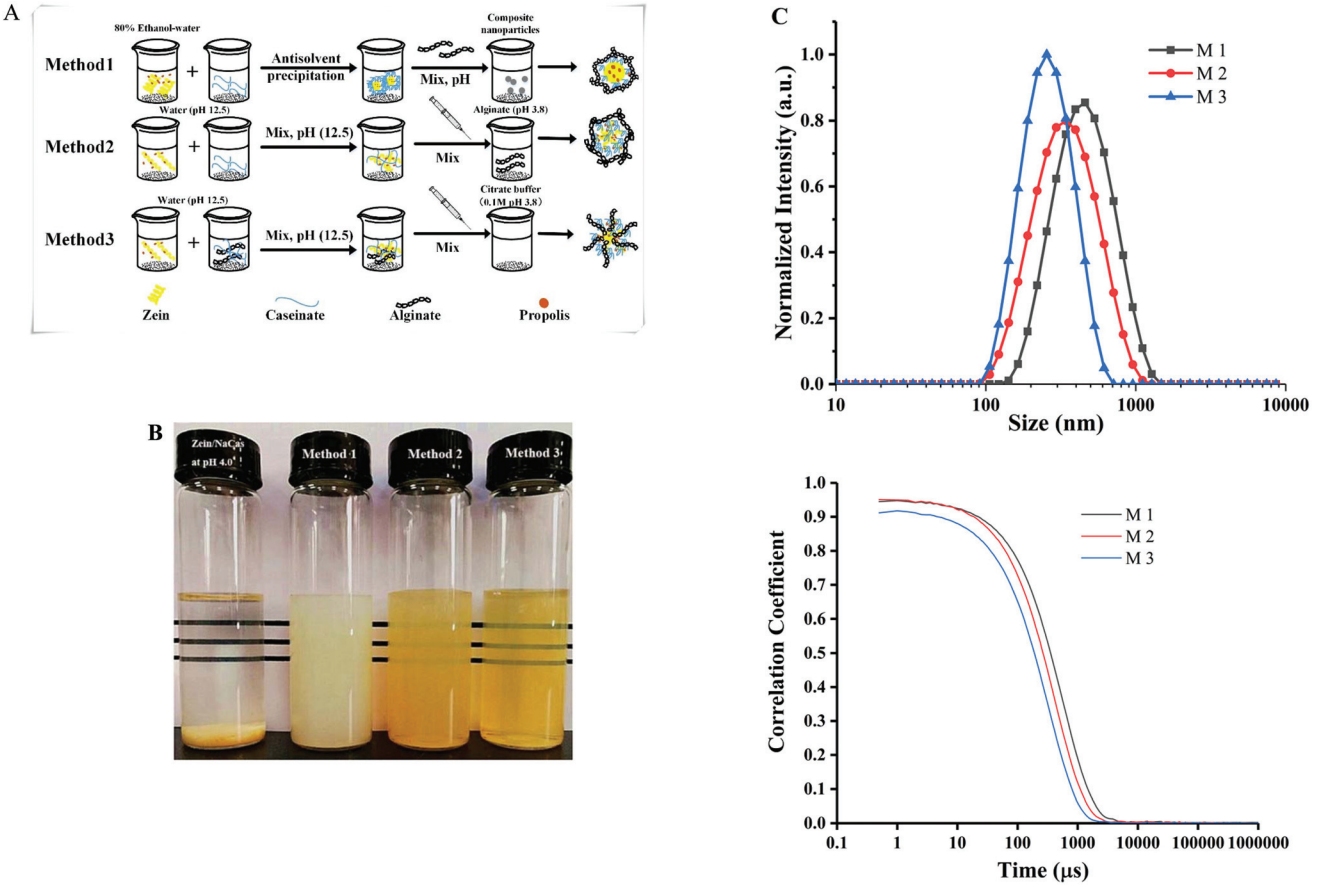

Fig. 1 (A) Schematic illustration of propolis loaded zein/NaCas/alginate nanoparticle fabrication using three different encapsulating approaches. (B) Appearance of zein/NaCas without alginate and nanoparticles prepared using three different encapsulating approaches after incubation at pH 12.5 for 30 min followed by acidification to pH 4.0. (C) Size distributions and correlation coefficient of pH 4.1 dispersions prepared with three different encapsulation approaches, after storage at 4 °C for 30 days.

tilled water adjusted to pH 4.0 was added to achieve a final volume of 25.0 mL. For Method 2, zein powder and NaCas powder were mixed with double distilled water with the pH adjusted to 12.5 using 3.0 M sodium hydroxide solution (NaOH) to prepare the zein (1%, w/v) and NaCas (1%, w/v) stock solutions, respectively. Sodium alginate (1%, w/v) was dissolved in double distilled water. Briefly, 1 mL of zein solution and 1 mL of NaCas solution were added into a glass vial containing 8 mL of double distilled water with the pH adjusted to 12.5 using 1.0 M NaOH to prepare a well-blended solution by stirring at 600 rpm for 30 min. Powdered propolis (5 mg) was then added into the mixture and stirred for 10 min. The resulting mixture was then poured in 15.0 mL of diluted sodium alginate solution (pH 3.8, 0.1 M citrate buffer) and stirred at 1500 rpm for 30 min, corresponding to zein : NaCas : alginate mass ratios of 1 : 1 : 1. For Method 3, dispersions with equal amounts of propolis, zein, NaCas, and alginate were also prepared, and all procedures were similar to Method 2 except that alginate solution was directly mixed with zein and NaCas under alkaline pH conditions for 30 min, instead of prediluting in 0.1 M citrate buffer at pH 3.8. The liquid dispersions with a final pH value of 4.1 ± 0.1 were stored in a refrigerator at 4 °C for further analysis or were freeze-dried for 24 h to obtain powders of nanoparticle dispersions for further characterization.

2.3. Determination of total phenolic contents

For the determination of total polyphenol contents in the propolis extract (PE) and nanoparticles, the Folin–Ciocalteu method[26] was employed with gallic acid as a standard. For this, appropriately diluted samples (1.0 mL) were mixed with 1.0 mL of the Folin–Ciocalteu reagent. After 5 min, 5.0 mL of Na_2CO_3 (1.0 M) solution was added and diluted to 10 mL using double distilled water. After shaking well, the mixture was incubated in the dark for 1 h, and the absorbance was read at 765 nm using a spectrophotometer (Shimadzu UV-2550). Quantification was performed using a standard curve of gallic acid at a concentration of 5–30 μg mL^{-1} (R^2 = 0.998). The total polyphenol content was expressed as milligram of gallic acid equivalent per gram of sample.

2.4. Nanoparticle characterization

The average particle size, zeta potential, and polydispersity index (PDI) of freshly prepared formulations were determined

using a combined dynamic light scattering and particle electrophoresis instrument (Zetasizer Nano-ZS90, Malvern Instruments Ltd, Worcestershire, UK). The particle size was calculated using the Stokes–Einstein equation. The zeta potential of nanoparticles was obtained using the Smoluchowski model through electrophoretic mobility measurements by laser Doppler velocimetry (Zetasizer Nano ZS90, Malvern, UK). The refraction index used here was 1.330. Samples were diluted 10 times using 0.1 M citrate buffer (pH 4.1) before measurement to avoid multiple particle effects. All samples were analyzed in triplicate at room temperature (25 °C). The FT-IR spectra of the samples were obtained at room temperature (25 °C) using an ATR-FTIR spectrophotometer (Nicolet iS10, Thermo-Scientific, WI, USA). The spectra were acquired at a wavenumber range from 400 to 4000 cm^{-1} with a 4 cm^{-1} resolution and accumulation of 32 scans. The microstructures of nanoparticles were determined using a transmission electron microscope (TEM, H-7650, Hitachi, Japan) operating at 80 kV and the sample was stained with 1% uranyl acetate.

2.5. Encapsulation efficiency (EE) and loading capacity (LC)

According to our previous study,[25] the EE (%) of propolis in the nanoparticles was calculated using eqn (1):

$$\text{EE}\ (\%) = (1 - \text{free propolis/total propolis}) \times 100 \quad (1)$$

where total propolis is the total content of polyphenol contained in the nanoparticle suspension and free propolis is the content of polyphenol obtained in the filtrate receiver after ultrafiltration (4000*g* for 50 min) using centrifugal filters (Ultrafree®-M 10 000 NMWL Filter Unit, Millipore, Cork, Ireland). The total and free polyphenol content was measured using the Folin–Ciocalteu method as described in section 2.3. The freeze-dried samples were weighed, and the LC was calculated as follows:

$$\text{LC} = (\text{encapsulated propolis/weight of nanoparticles}) \times 100. \quad (2)$$

2.6. Stability to environmental conditions

Influence of sodium alginate concentration. Different sodium alginate concentrations may tailor particular characteristics of the propolis loaded nanoparticles. A series of nanoparticle suspensions with alginate concentrations ranging from 0 to 1.50 (mg mL^{-1}) were prepared and measured for particle size using dynamic light scattering.

Influence of pH and ionic strength. The pH (2.0, 3.0, 4.0, 4.5, 5.0, 6.0, 7.0, 8.0) and/or ionic strength (0, 100, 200, 300, 400 mM) of the nanoparticle suspensions were adjusted to various values and the stability of the nanoparticles to aggregation was examined using dynamic light scattering measurements.

2.7. *In vitro* digestion profile and bioaccessibility

The *in vitro* release profiles and bioaccessibility of free and encapsulated propolis were evaluated using *in vitro* simulated gastric fluid (SGF) and simulated intestinal fluid (SIF), as described in previous reports with slight modifications.[25,27,28] The composition of the simulated gastric and intestinal fluids is presented in Table 2. Ten milliliters of freshly prepared propolis loaded nanoparticle samples were first incubated in an equal volume of SGF. The mixture was maintained at constant pH and temperature (pH 3.0, 37 °C) with mild stirring for 2 h. After 120 min, the pH of the digestive production was raised to 7.0 using 2.0 M NaOH, 20 mL of preheated intestinal fluid was added and digested for 4 h at 37 °C under mild stirring. To calculate the accumulative percentage of released propolis in designated digestion times, the digesta was withdrawn (1 mL) at different time intervals (10, 30, 60, 90, 120, 150, 180, 240, 300, 360), 4.0 mL of PBS was added and subjected to centrifugation (4000*g*, 50 min) using an ultrafiltration device. Then, the polyphenol content in the filtrate which represented released propolis was measured using the Folin–Ciocalteu method after diluting appropriately with PBS. In addition, propolis (5 mg) dissolved in ethanol (0.5 mL, 10 mg mL^{-1}) was add to digestion solution (9.5 mL gastric fluid) as a blank control. After intestinal digestion was completed, the raw digesta from each sample was centrifuged at 15 000*g* for 1 h and the mixed micelle phases (clear supernatant) were collected in which propolis was solubilized. The propolis concentration was measured according to section 2.3. The propolis concentration in the mixed micelle phases (C_{micell}) as a percentage of the propolis concentration in the overall digesta at the end of the simulated GIT model ($C_{\text{overall digesta}}$) was defined as the *in vitro* bioaccessibility of propolis using the following equation:

$$\text{Bioaccessibility}\ (\%) = C_{\text{micell}}/C_{\text{overall digesta}} \times 100 \quad (3)$$

2.8. Statistical analysis

All experiments were performed in triplicate and the results were represented by mean ± standard error. Experimental statistics were performed by Duncan's test and differences with $P < 0.05$ were defined as statistically significant.

3. Results and discussion

3.1. Preparation and characterization of propolis loaded nanoparticles

According to our previous study, encapsulation of propolis into zein/carboxymethyl chitosan nanoparticles offered a promising approach to improve their solubility and bioavailability.[25] However, the different loading techniques that would affect the particulate characteristics of zein-based composite nanoparticles have not been reported yet. As shown in Fig. 1A, the method 1 loading technique is similar to the conventional anti-solvent precipitation method to fabricate zein/caseinate/alginate nanoparticles. In method 2 and method 3, an innovative pH-induced one-step assembly method was employed to encapsulate propolis into zein/caseinate/alginate nanoparticles; however the sequence of adding alginate was

different. The photographic images presented in Fig. 1B show that zein/NaCas nanoparticles without the addition of alginate were completely unstable and precipitated at pH 4.0. The dispersions prepared with alginate using the three methods did not show visible precipitates after one month of storage at 4 °C. The phenomenon indicated that alginate interacted with zein/NaCas nanoparticles and enhanced electrostatic and steric repulsion against aggregation.[15] It was noted that the dispersions prepared using method 2 and method 3 had an orange-yellow color. A similar observation was reported by a previous study, showing that the color of clove bud oil became darker after heating and alkaline treatment.[29] The effect of the pH cycle (alkaline dissolution and acidification) on the change of biological activity and stability of propolis components is discussed in ESI Fig. S1.† Interestingly, as shown in Table 1, the zein/NaCas/alginate nanoparticles fabricated by method 1 had a larger particle size than those fabricated by pH-induced one-step assembly methods (method 2 and method 3) without using ethanol as a loading solvent for zein and propolis. Meanwhile, the method 2 and method 3 samples exhibited a smaller PDI value than the method 1 sample. These observations corresponded to the intensity weighted particle size distributions of all dispersions after storage at 4 °C for 30 days (Fig. 1C). All the three dispersions were monomodal, while the method 1 sample showed majority of the particles around larger particle sizes than the ones prepared using method 2 and method 3. Thus, the pH-induced one-step assembly method could be an effective method for the preparation of zein/NaCas/alginate nanoparticles with a smaller particle size and narrower particle size distribution. This speculation is in accordance with previous studies which have shown that the pH-driven loading method has resulted in curcumin loaded solid lipid nanoparticles with a smaller particle size and acceptable homogeneity.[30] It is worth mentioning that the zeta potential of nanoparticles prepared using the pH-induced one-step assembly method (method 2 and method 3) was significantly less negative than that of those prepared using the conventional anti-solvent precipitation method (method 1) while the method 3 sample exhibited the lowest zeta potential (Table 1). These observations indicated that the structure of nanoparticles prepared using method 2 or method 3 changed significantly compared to nanoparticles prepared using method 1. Similar phenomena have also been observed by other researchers.[12,13] This could be due to the complete mixing of the protein and alginate and coalition to form discrete nanoparticles with clear partition and part of the negatively charged polysaccharide chains buried in the core of the zein/NaCas/alginate nanoparticles.[13] Therefore, compared to other nanoparticles, the zeta potential of the nanoparticles (method 3) significantly decreased.

Table 1 Comparisons of size, PDI, count rate, zeta potential and encapsulation efficiency of colloidal particles produced with equal masses of zein, NaCas and alginate using three different methods. The propolis concentration was 0.25 mg mL^{-1}

Treatment	Method 1	Method 2	Method 3
Size (nm)	362.2 ± 1.5^{c}	267.4 ± 1.5^{b}	208.1 ± 2.1^{a}
PDI	0.26 ± 0.01^{b}	0.24 ± 0.00^{a}	0.23 ± 0.02^{a}
Count rate (kcps)	175.6 ± 0.4^{b}	144.9 ± 0.3^{a}	268.2 ± 1.2^{c}
Zeta potential (mV)	-31.7 ± 0.8^{a}	-28.0 ± 0.8^{b}	-26.9 ± 0.5^{c}
EE (%)	76.2 ± 0.6^{a}	82.4 ± 1.3^{b}	86.5 ± 0.7^{c}
LC (μg mg^{-1})	43.6 ± 2.2^{a}	54.2 ± 1.2^{b}	59.6 ± 1.5^{c}

Numbers are mean ± standard deviation (n = 3). Different superscript letters in the same row indicate significant differences ($P < 0.05$). Please refer to Fig. 1A for detailed information on the different methods.

Table 2 Final concentrations of constituents before addition to the sample of the simulated gastric and intestinal fluids

Constituent	Simulated gastric fluid (pH 3.0) mmol L^{-1}	Simulated intestinal fluid (pH 7.0)
KCl	5.52	5.44
KH_2PO_4	0.72	0.64
$NaHCO_3$	20.00	68.00
NaCl	37.76	30.72
$MgCl_2(H_2O)_6$	0.08	0.26
$(NH_4)_2CO_3$	0.40	
NaOH		3.73
HCl	22.48	6.72
$CaCl_2(H_2O)_2$	0.07	0.30
	mg mL^{-1}	
Tween 20	0.5	
Pepsin	10	
Pancreatin		30
Bile extract		6.25

The count rate plays a vital role in indicating the number and concentration of colloidal nanoparticles, which is proportional to the sixth power of particle size as well as their number.[30,31] Interestingly, the method 3 sample exhibited the highest count rate as well as the smallest particle size among the formulations (Table 1). According to a previous study,[31,32] these results implied that smaller nanoparticles were formed in greater number by method 3. The NTA data (Fig. S2†) further supported the count rate data in DLS (Table 1). Most notably, the nanoparticles prepared by method 3 exhibited the highest encapsulation efficiency compared to the other two methods while the corresponding loading capacity increased from around 43.6 μg mg^{-1} to around 59.6 μg mg^{-1} (Table 1). All of these are compelling evidence to support the fact that the pH-induced one-step assembly method is a promising approach to encapsulate propolis into zein nanoparticles modified by NaCas and alginate, and that interaction of alginate with the protein (zein and NaCas) under alkaline conditions is critical to formulate the most compact and homogeneous propolis loaded zein/NaCas/alginate nanoparticles (method 3 sample).

3.2. Effect of NaCas/alginate mass ratio

Fig. 2 shows the effect of the mass ratio of NaCas/alginate (8 : 1, 4 : 1, 2 : 1, 4 : 3, 1 : 1, 4 : 5, and 2 : 3) on the particle size and PDI at fixed concentrations of zein (1.0 mg mL^{-1}) and

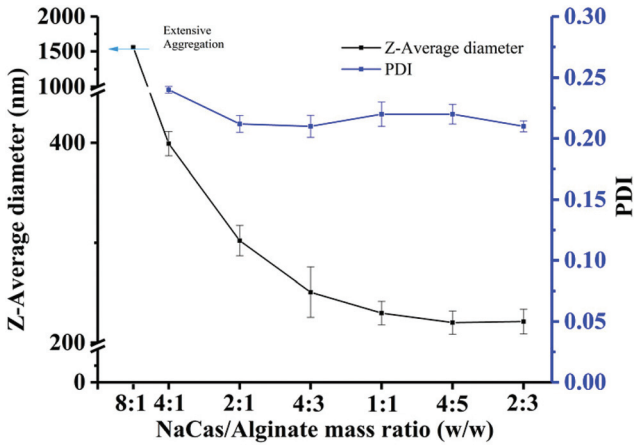

Fig. 2 Effect of NaCas/alginate mass ratio on the *Z*-average diameter and PDI of zein/NaCas/alginate nanoparticles (method 3 sample). Data represent the mean ± standard deviation (SD, n = 3).

NaCas (1.0 mg mL^{-1}), and pH 4.1. Notably, extensive particle aggregation occurred when the NaCas/alginate mass ratio was higher than the ratio of 4 : 1, suggesting that insufficient alginate molecules covered the zein/NaCas nanoparticles.[14] The particle size remained relatively constant at higher alginate concentration, corresponding to a NaCas/alginate mass ratio of 1 : 1 to 2 : 3. This phenomenon indicated that the zein/NaCas nanoparticles were saturated with alginate at these higher alginate levels.[14] For the effect of alginate on the particle count rate, the particle count rate at a NaCas/alginate mass ratio of 4 : 1 was the lowest (146.75 kcps). As alginate increased to a higher concentration, the count rate of particles increased and was higher at a higher alginate/NaCas mass ratio (data not shown). Because the NaCas concentration was kept unaltered in sample fabrication and the amount of alginate was higher at a higher alginate/NaCas mass ratio, the higher count rate suggests the formation of a greater population of nanoparticles. A previous study by Luo *et al.*[18] has also described this phenomenon. The nanoparticles (NaCas/alginate mass ratio of 4 : 1–2 : 3) exhibited a small PDI (0.21–0.24), suggesting that particles may have a more uniform size. For the reason of small particle size, high stability and ease of fabrication, NaCas/alginate with a mass ratio of 1 : 1 was selected to develop propolis loaded zein/NaCas/alginate nanoparticles in further experiments using the pH-induced one-step assembly method (method 3).

3.3. Morphological observation

To observe the morphology of the zein/NaCas complex and propolis loaded zein/NaCas/alginate nanoparticles, the TEM images of four samples were obtained and are presented in Fig. 3. The zein/NaCas complex without alginate formed large aggregates due to their poor aggregation stability near the NaCas isoelectric pH, which agreed with the photographic images presented in Fig. 1B. When alginate was added, the three nanoparticle samples showed spherical appearance, and the method 1 sample showed a larger size than the method 2 and method 3 samples. The nanoparticles (method 2 sample) were clumped to each other, which might be attributed to the alginate coating on the surface of zein/NaCas nanoparticles.[33] Interestingly, the nanoparticles (method 3 sample) appeared spherical and exhibited smooth surfaces with clearer partition among each other. Overall, nanoparticles formed with method 3 were more homogeneous, more discrete, and smaller than those of method 2, suggesting that most alginates were probably involved in nanoparticle fabrication in method 3 but adsorbed on the surface of zein/NaCas nanoparticles in method 2.[17] The TEM technique can also distinguish the localization of different materials in the sample according to the difference in the material density without using fluorescent tagging.[34] As shown in Fig. 3 (M1), the core–shell structure was clearly observed with the shell being more electron dense as compared to the core (marked with red arrows), which was in agreement with published results.[35]

3.4. FTIR analysis

In this study, the intermolecular interaction between propolis and nanoparticles was revealed by FTIR (Fig. 4). The pure propolis spectrum showed a peak at 3362 cm^{-1} related to phenolic compounds and carbohydrates[36] (Fig. 4A). Propolis exhibited two characteristic peaks at 2927 and 2854 cm^{-1}, respectively, which are attributed to hydrocarbon stretching vibration. The two peaks at 1639 and 1513 cm^{-1} are generated by ν(C=O), ν(C=C), and δ_{as}(N–H), which are shown in aromatic compounds, for instance, flavonoids.[36,37] The band at 1500 to 1000 cm^{-1} is mostly contributed by the presence of flavonoids, lipid, and alcohols.[36] For zein (Fig. 4A), the peak at 3317 cm^{-1} corresponded to –OH stretching. Two peaks located at 1655 cm^{-1} and 1535 cm^{-1} corresponded to C=O stretching (amide I) and N–H bending and stretching of C–N (amide II), respectively.[25] The FTIR spectrum of NaCas displayed a peak for –OH stretching at 3316 cm^{-1}, and two characteristic peaks for amide I and amide II bonds in the range of 1500–1700 cm^{-1} (1654 cm^{-1} and 1535 cm^{-1}).[38] The peaks in the spectrum of alginate at around 3500–3000, 1609, 1413, and 1032 cm^{-1} represented the –OH stretch, the asymmetrical stretch of –COOH, the symmetrical stretch of –COOH, and the COH stretch, respectively.[39] Characteristic aromatic rings of flavonoids existed in propolis absorption peaks at 1162 cm^{-1} and 1031 cm^{-1}, which were shifted to 1159 cm^{-1} and 1021 cm^{-1} in the spectrum of propolis loaded zein nanoparticles (NPs) (Fig. 4B). This indicated that hydrophobic interactions occurred between zein and propolis.[25] By comparing the spectra of zein and propolis loaded zein NPs (Fig. 5B), it was found that the adsorption peak of amide II (C–N stretching and N–H bending) was shifted from 1535 cm^{-1} in zein to 1516 cm^{-1} in propolis loaded zein NPs which was the sign of the formation of hydrogen bonds between zein and propolis *via* the N–H bond in zein.[40] After the formation of zein/NaCas/alginate NPs, the characteristic peaks of the asymmetrical stretch at 1609 cm^{-1} (–COOH) of alginate and the $-NH_3^+$ bending vibrations (1535 cm^{-1}) of the protein (zein, NaCas)

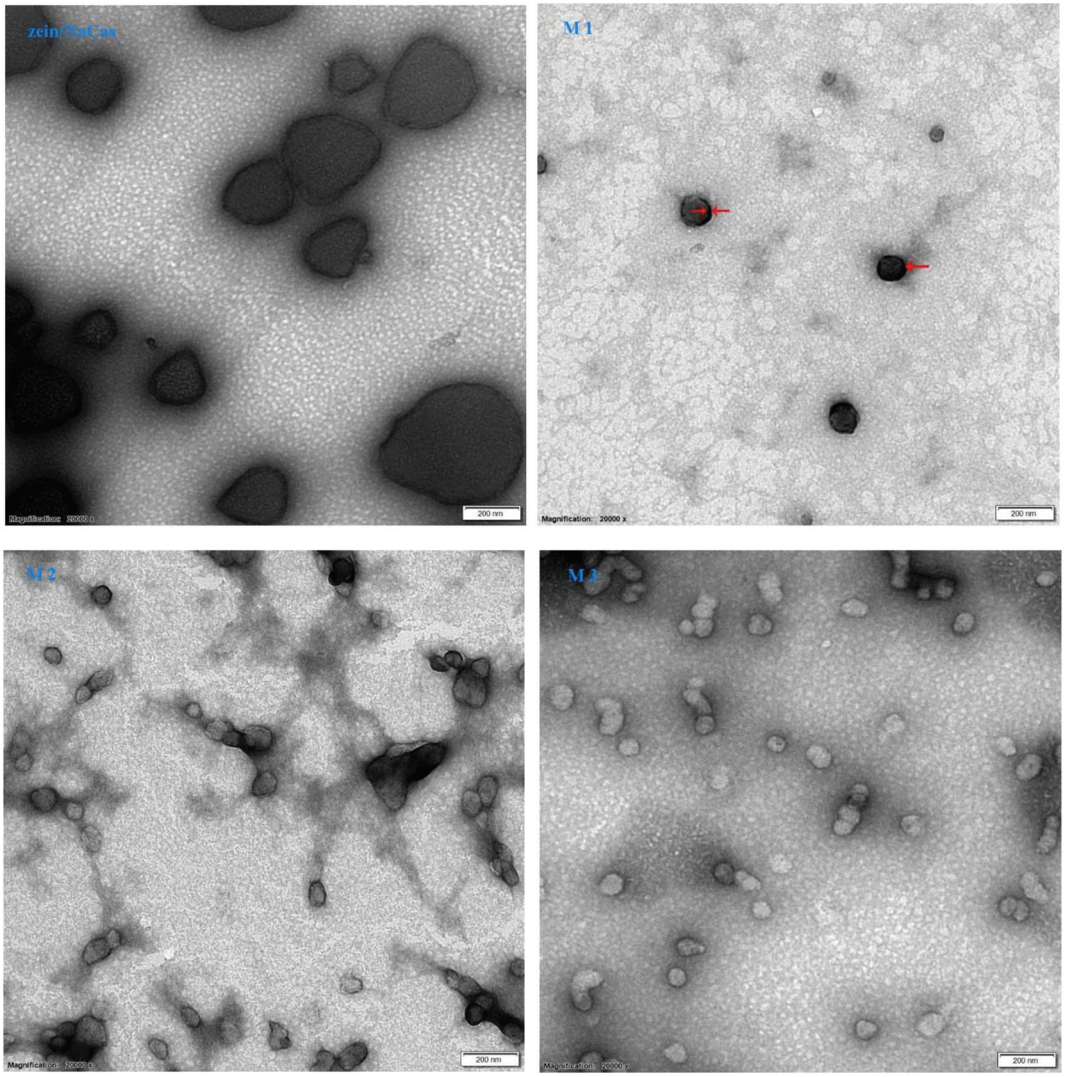

Fig. 3 TEM images of zein/NaCas without alginate and nanoparticles produced using three different loading methods.

were not observable (Fig. 4B). It was revealed that zein, NaCas and alginate can form stable polyelectrolyte complex nanoparticles through electrostatic interactions.[16] More interestingly, the propolis loaded zein/NaCas/alginate NPs showed the same FTIR spectrum as that of the blank nanoparticles around 1718, 1599, 1401, and 1234 cm^{-1}. This finding suggested that the primary structure of the zein/NaCas/alginate NPs was virtually unchanged after propolis encapsulation.[41] Encapsulation of propolis was revealed by the result that the majority of the characteristic peaks of propolis were overlapped by the absorption peaks of the nanoparticle matrix.[25]

3.5. Stability of propolis nanoparticles

Fig. 5A shows that the propolis loaded zein/NaCas/alginate nanoparticles appeared to be stable against aggregation across the entire pH range studied, especially near the isoelectric point pH of the NaCas (pI, around pH 4.5) and zein (pI, around pH 6.2). The good aggregation stability of the nanoparticles can be attributed to a strong steric stabilization and electrostatic repulsion between them due to effective coverage of alginate on the surface of zein/NaCas.[15,42] However, the particle size increased when the pH was reduced to 3.0 and 2.0 (Fig. 5A). Meanwhile, the magnitude of the zeta potential decreased significantly from −29.5 ± 0.32 mV at pH 4.0 to −6.6 ± 0.25 mV at pH 2.0 ($p < 0.05$) (Fig. 5B). The particle size increased at pH 2 due to the reduction in the electrostatic repulsion between the particles.[14] Indeed, carboxylic groups on the alginate molecules have pK_a values around pH 3.5. Consequently, at pH 2, protonation of the carboxyl groups on the alginate molecules occurred and they lose their negative charge ($-COO^-$).[14] On the other hand, at low pH values, the net charge on the biopolymer particles becomes less negative also due to net-positively charged protein components (pH < pI, protonation of some amino acids of the protein) complexing with free alginate.[43] At pH between 6 and 8, the particle size decreased appreciably (Fig. 5A). This result should be ascribed to the dissociation of the nanoparticles at high pH values where both the protein (zein and NaCas) and alginate

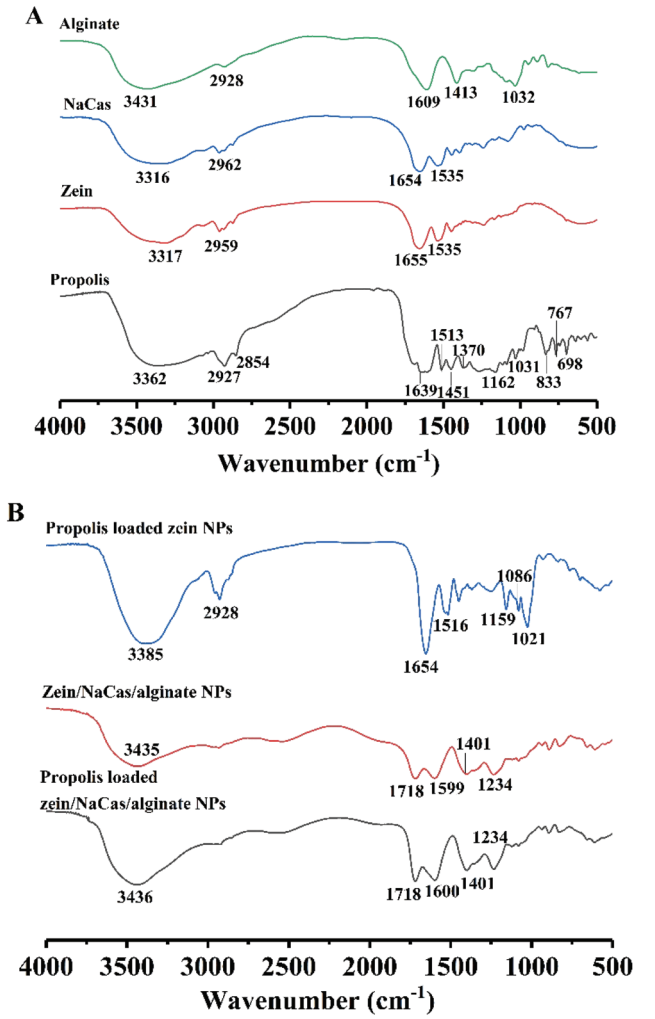

Fig. 4 Fourier transform infrared spectrum of (A) individual polymers and (B) propolis loaded zein nanoparticles (NPs); zein/NaCas/alginate nanoparticles; and propolis loaded zein/NaCas/alginate nanoparticles (method 3 sample).

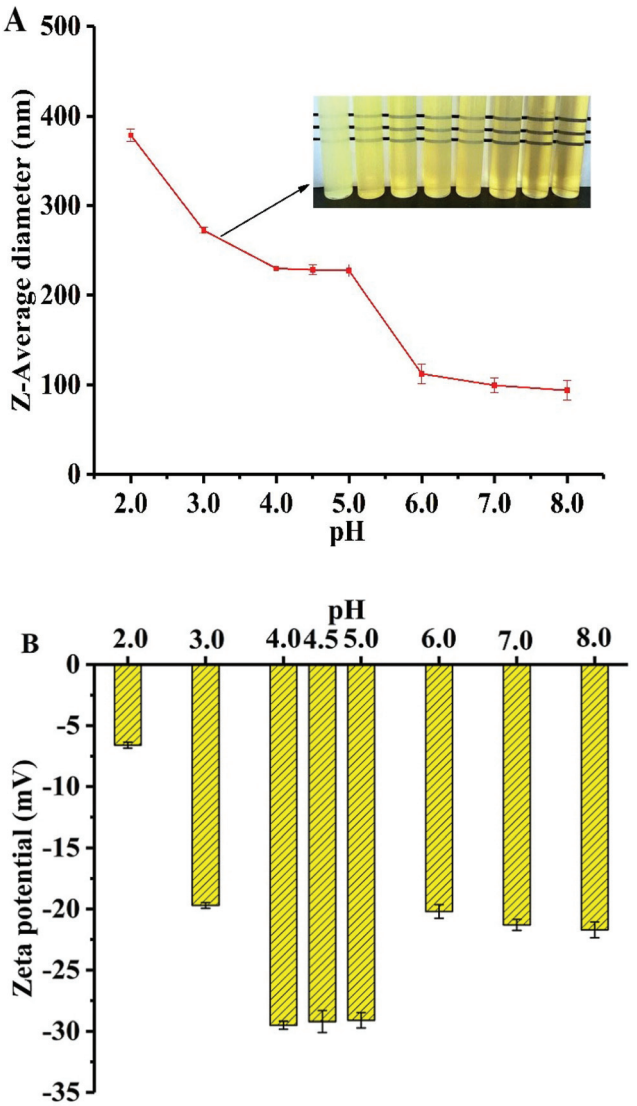

Fig. 5 Effect of pH on the (A) *Z*-average diameter, (B) zeta potential, and appearance of propolis loaded zein/NaCas/alginate nanoparticles (method 3 sample).

have the same charge (negative charge) and repel each other.[15] Therefore, zein/NaCas/alginate nanoparticles may be a promising vehicle for pH-triggered release of propolis. Interestingly, when the pH was increased from 4.0 to 8.0, the surface charge of propolis loaded nanoparticles decreased from −29.5 ± 0.32 to −21.7 ± 0.65 mV. This phenomenon might be related to the shielding effect caused by the excess free biopolymers (dissociation of the nanoparticles) around the nanoparticles (Fig. 5B).[44] The influence of ionic strength on the stability of the propolis loaded zein/NaCas/alginate nanoparticles (method 3 sample) is presented in Fig. 6. It could be observed from Fig. 6A that the propolis nanoparticles had no visible changes in their visual appearance and *Z*-average diameter at low NaCl concentration (≤200 mM), but aggregation was observed at high NaCl concentration (≥400 mM NaCl). The finding suggested that the nanoparticles were unstable at higher ionic strength. This phenomenon was due to the ability of the sodium cations to accumulate around the surface of anionic propolis nanoparticles and shield the electrostatic repulsion between them, thereby leading to aggregation.[19] The conclusion was supported by zeta potential analysis (Fig. 6B), which indicated that the zeta potential value decreased with the rise of ionic strength (from −34 to −20 mV for propolis nanoparticles). Surprisingly, the propolis nanoparticles were unstable to aggregation at high salt levels, which is in contrast to earlier studies on NaCas coated zein nanoparticles (stability at 1.5 M NaCl).[42] This discrepancy may be attributed to the difference in the structure of nanoparticles (core–shell *vs.* well mixing and hybrids).[12]

3.6. *In vitro* release profile and bioaccessibility of propolis

As shown in Fig. 7A, only 33% of free propolis diffused into the simulated gastrointestinal tract (SGI) within 6 h of incubation due to the poor solubility of propolis in an aqueous

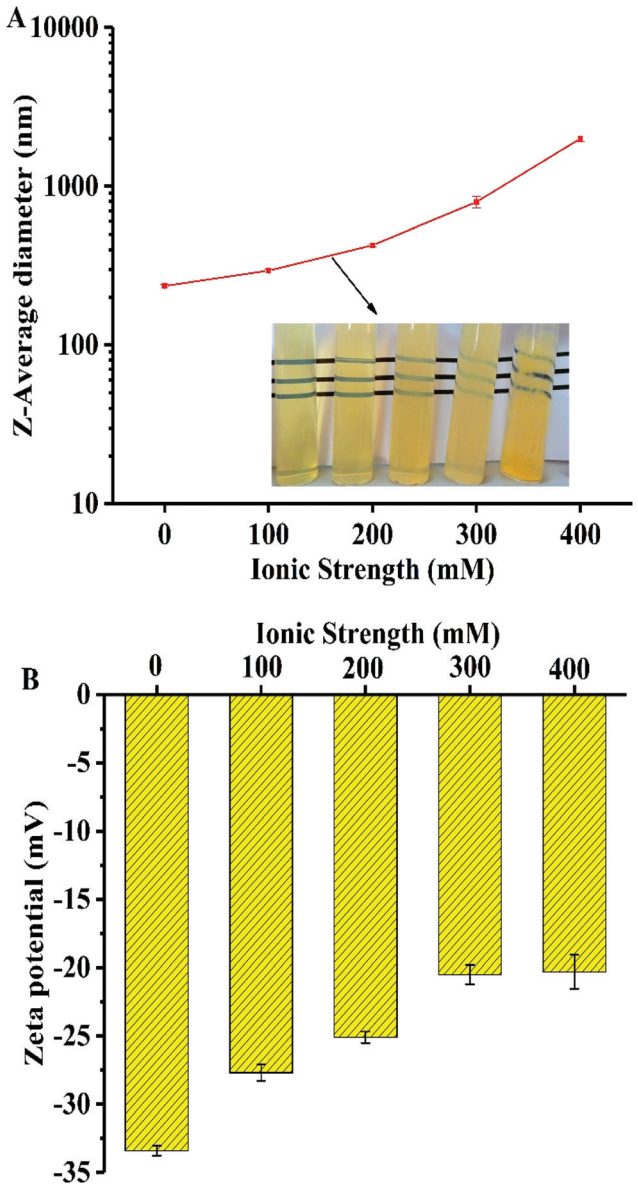

Fig. 6 Effect of NaCl concentration on the (A) *Z*-average diameter, (B) zeta potential, and appearance of propolis loaded zein/NaCas/alginate nanoparticles (method 3 sample).

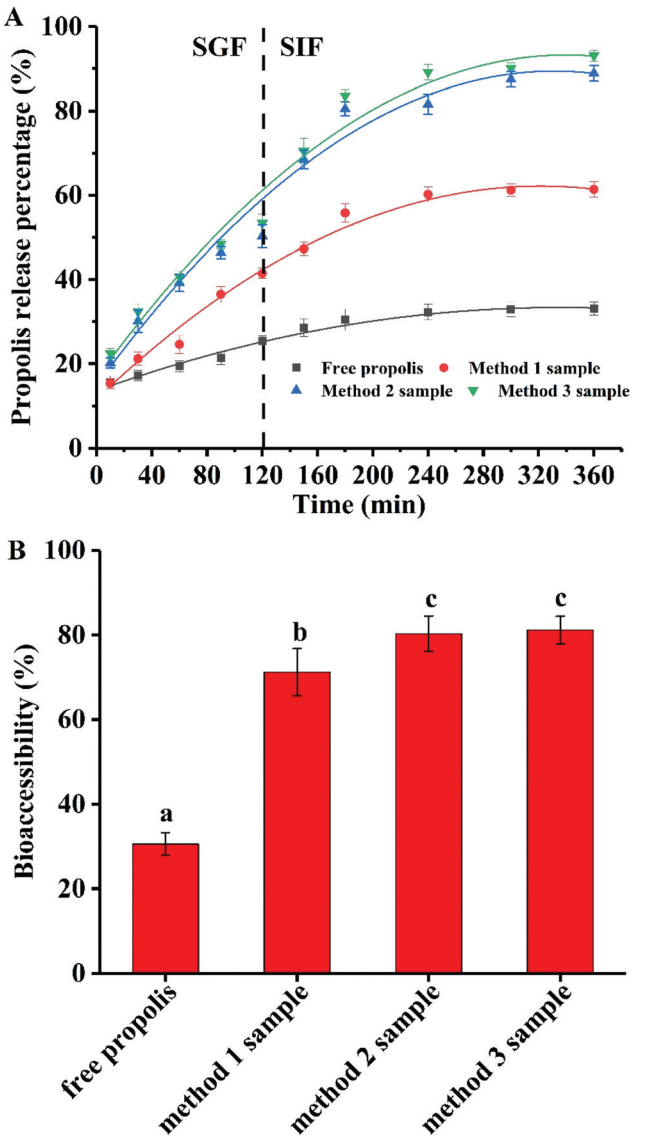

Fig. 7 (A) *In vitro* dissolution profiles of free and encapsulated propolis in SGF and SIF. (B) *In vitro* bioaccessibility of free propolis and encapsulated propolis in three different nanoparticles.

solution. This kinetics was in accordance with the release of resveratrol, as shown in a previous study.[28] Nevertheless, propolis released approximately 60% (method 1 sample) and 90% (method 2 and method 3 samples) under SGI conditions, respectively. Propolis in method 2 and method 3 samples presented a similar kinetic release profile throughout SGI. Notably, compared to the method 1 sample, a more significant burst effect in the method 2 and method 3 samples was detected after 4 h of SGI digestion. These findings may be due to the intestinal pH value (around pH 7.0) leading to the dissociation of the nanoparticles, which was in favour of the enzymatic degradation of nanoparticles during intestinal digestion. This phenomenon was also observed in section 3.5. Subsequently, the bioaccessibility of propolis after being exposed to the small intestine phase was determined (Fig. 7B). Mixing propolis with an aqueous solution would cause the formation of precipitates immediately, which might result in propolis exhibiting lower bioaccessibility (around 30%). Nevertheless, the bioaccessibility of propolis was still around 30%. It can be explained that polyphenols interact with the protein (such as enzymes) present in the gastric and intestinal fluids increasing their solubility in the micelle phase.[45] As expected, the bioaccessibility of propolis encapsulated in zein/NaCas/alginate nanoparticles was markedly improved by 70% and 80% compared to free propolis (around 30%). The binding between propolis and the nanoparticles through hydrogen bonds and electrostatic and hydrophobic interactions enhanced the content of propolis in the micellar

phase. These results indicate that zein/NaCas/alginate nanoparticles are a promising oral delivery system for propolis.

4. Conclusions

In summary, propolis loaded zein/NaCas/alginate nanoparticles were successfully prepared using a pH-induced one-step assembly method to enhance its bioaccessibility. Three different methods to load propolis into zein/NaCas/alginate nanoparticles were advised and compared for their effects on the physicochemical properties of the resultant nanoparticles. Compared to the nanoparticles prepared using method 1, zein/NaCas/alginate nanoparticles prepared using method 3 show smaller average particle size and higher encapsulation efficiency and loading capacity. These nanoparticles were shown to be stable against aggregation over a wide range of pH values (2–8) and salt concentrations (0–300 mM NaCl). This study suggested that a low-energy, pH-induced one-step assembly method could potentially be used to fabricate zein-based vehicles without using organic solvents and specific equipment to broaden the applications of propolis and other bioactive compounds in the food, cosmetic, and pharmaceutical industries.

Conflicts of interest

There are no conflicts to declare.

Acknowledgements

Financial support from the Natural Science Foundation of Zhejiang Province (LY18C200003) and Zhejiang Provincial Top Key Discipline of Food Science and Biotechnology is acknowledged. The authors thank Dr Rituja Upadhyay for proofreading of the research article.

References

1 P. Argos, K. Pedersen, M. D. Marks and B. A. Larkins, A structural model for maize zein proteins, *J. Biol. Chem.*, 1982, **257**, 9984–9990.
2 L. Wang and Y. Zhang, Eugenol Nanoemulsion Stabilized with Zein and Sodium Caseinate by Self-Assembly, *J. Agric. Food Chem.*, 2017, **65**, 2990–2998.
3 M. Wang, Y. Fu, Y. Shi, G. Chen, X. Li, H. Zhang and Y. Shen, Fabrication and characterization of carboxymethyl chitosan and tea polyphenols coating on zein nanoparticles to encapsulate β -carotene by anti-solvent precipitation method, *Food Hydrocolloids*, 2017, **77**, 577–587.
4 Y. Wei, C. Sun, L. Dai, X. Zhan and Y. Gao, Structure, physicochemical stability and in vitro simulated gastrointestinal digestion properties of β-carotene loaded zein-propylene glycol alginate composite nanoparticles fabricated by emulsification-evaporation method, *Food Hydrocolloids*, 2018, **81**, 149–158.
5 A. Patel, Y. Hu, J. K. Tiwari and K. P. Velikov, Synthesis and characterisation of zein–curcumin colloidal particles, *Soft Matter*, 2010, **6**, 6192–6199.
6 L. Dai, R. Li, Y. Wei, C. Sun, L. Mao and Y. Gao, Fabrication of zein and rhamnolipid complex nanoparticles to enhance the stability and in vitro release of curcumin, *Food Hydrocolloids*, 2018, **77**, 617–628.
7 C. Sun, Y. Wei, R. Li, L. Dai and Y. Gao, Quercetagetin-Loaded Zein-Propylene Glycol Alginate Ternary Composite Particles Induced by Calcium Ions: Structure Characterization and Formation Mechanism, *J. Agric. Food Chem.*, 2017, **65**, 3934–3945.
8 K. Hu, X. Huang, Y. Gao, X. Huang, H. Xiao and D. J. McClements, Core-shell biopolymer nanoparticle delivery systems: synthesis and characterization of curcumin fortified zein-pectin nanoparticles, *Food Chem.*, 2015, **182**, 275–281.
9 Q. Zhong and M. Jin, Zein nanoparticles produced by liquid–liquid dispersion, *Food Hydrocolloids*, 2009, **23**, 2380–2387.
10 H. Chen and Q. Zhong, A novel method of preparing stable zein nanoparticle dispersions for encapsulation of peppermint oil, *Food Hydrocolloids*, 2015, **43**, 593–602.
11 C. Sun, Y. Gao and Q. Zhong, Effects of acidification by glucono-delta-lactone or hydrochloric acid on structures of zein-caseinate nanocomplexes self-assembled during a pH cycle, *Food Hydrocolloids*, 2018, **82**, 173–185.
12 K. Pan and Q. Zhong, Low energy, organic solvent-free co-assembly of zein and caseinate to prepare stable dispersions, *Food Hydrocolloids*, 2016, **52**, 600–606.
13 T. Wang, M. Yue, P. Xu, R. Wang and Z. Chen, Toward water-solvation of rice proteins via backbone hybridization by casein, *Food Chem.*, 2018, **258**, 278–283.
14 K. Hu and D. J. McClements, Fabrication of biopolymer nanoparticles by antisolvent precipitation and electrostatic deposition: Zein-alginate core/shell nanoparticles, *Food Hydrocolloids*, 2015, **44**, 101–108.
15 W. Liu, J. Wang, D. J. McClements and L. Zou, Encapsulation of β-carotene-loaded oil droplets in caseinate/alginate microparticles: Enhancement of carotenoid stability and bioaccessibility, *J. Funct. Foods*, 2018, **40**, 527–535.
16 W. Liu, J. Liu, W. Liu, T. Li and C. Liu, Improved physical and in vitro digestion stability of a polyelectrolyte delivery system based on layer-by-layer self-assembly alginate-chitosan-coated nanoliposomes, *J. Agric. Food Chem.*, 2013, **61**, 4133–4144.
17 C. Sun, Y. Gao and Q. Zhong, Properties of Ternary Biopolymer Nanocomplexes of Zein, Sodium Caseinate, and Propylene Glycol Alginate and Their Function of Stabilizing High Internal Phase Pickering Emulsions, *Langmuir*, 2018, **34**, 9215–9227.
18 Y. Luo, K. Pan and Q. Zhong, Casein/pectin nanocomplexes as potential oral delivery vehicles, *Int. J. Pharm.*, 2015, **486**, 59–68.
19 S. Peng, Z. Li, L. Zou, W. Liu, C. Liu and D. J. McClements, Enhancement of Curcumin Bioavailability by Encapsulation

in Sophorolipid-Coated Nanoparticles: An in Vitro and in Vivo Study, *J. Agric. Food Chem.*, 2018, **66**, 1488–1497.
20 K. Pan, Y. Luo, Y. Gan, S. J. Baek and Q. Zhong, pH-driven encapsulation of curcumin in self-assembled casein nanoparticles for enhanced dispersibility and bioactivity, *Soft Matter*, 2014, **10**, 6820–6830.
21 K. Pan, H. Chen, S. J. Baek and Q. Zhong, Self-assembled curcumin-soluble soybean polysaccharide nanoparticles: Physicochemical properties and in vitro anti-proliferation activity against cancer cells, *Food Chem.*, 2018, **246**, 82–89.
22 O. Catchpole, K. Mitchell, S. Bloor, P. Davis and A. Suddes, Anti-gastrointestinal cancer activity of cyclodextrin-encapsulated propolis, *J. Funct. Foods*, 2018, **41**, 1–8.
23 C.-H. Yen, H.-F. Chiu, C.-H. Wu, Y.-Y. Lu, Y.-C. Han, Y.-C. Shen, K. Venkatakrishnan and C.-K. Wang, Beneficial efficacy of various propolis extracts and their digestive products by in vitro simulated gastrointestinal digestion, *LWT–Food Sci. Technol.*, 2017, **84**, 281–289.
24 B. Bueno-Silva, P. L. Rosalen, S. M. Alencar and M. P. A. Mayer, Anti-inflammatory mechanisms of neovestitol from Brazilian red propolis in LPS-activated macrophages, *J. Funct. Foods*, 2017, **36**, 440–447.
25 H. Zhang, Y. Fu, F. Niu, Z. Li, C. Ba, B. Jin, G. Chen and X. Li, Enhanced antioxidant activity and in vitro release of propolis by acid-induced aggregation using heat-denatured zein and carboxymethyl chitosan, *Food Hydrocolloids*, 2018, **81**, 104–112.
26 R. M. Lamuela-Raventós, V. L. Singleton and R. Orthofer, Analysis of Total Phenols and Other Oxidation Substrates and Antioxidants by Means of Folin-Ciocalteu Reagent, *Methods Enzymol.*, 1999, **299**, 152–178.
27 G. Davidov-Pardo, S. Perez-Ciordia, M. R. Marin-Arroyo and D. J. McClements, Improving resveratrol bioaccessibility using biopolymer nanoparticles and complexes: impact of protein-carbohydrate maillard conjugation, *J. Agric. Food Chem.*, 2015, **63**, 3915–3923.
28 W. Xiong, C. Ren, J. Li and B. Li, Enhancing photostability and bioaccessibility of resveratrol using ovalbumin-carboxymethylcellulose nanocomplexes and nanoparticles, *Food Funct.*, 2018, **9**, 3788–3797.
29 Y. Luo, Y. Zhang, K. Pan, F. Critzer, P. M. Davidson and Q. Zhong, Self-Emulsification of Alkaline-Dissolved Clove Bud Oil by Whey Protein, Gum Arabic, Lecithin, and Their Combinations, *J. Agric. Food Chem.*, 2014, **62**, 4417–4424.
30 J. Xue, T. Wang, Q. Hu, M. Zhou and Y. Luo, Insight into natural biopolymer-emulsified solid lipid nanoparticles for encapsulation of curcumin: Effect of loading methods, *Food Hydrocolloids*, 2018, **79**, 110–116.
31 Z. Teng, Y. Luo and Q. Wang, Carboxymethyl chitosan–soy protein complex nanoparticles for the encapsulation and controlled release of vitamin D3, *Food Chem.*, 2013, **141**, 524–532.
32 Z. Teng, Y. Luo and Q. Wang, Nanoparticles synthesized from soy protein: preparation, characterization, and application for nutraceutical encapsulation, *J. Agric. Food Chem.*, 2012, **60**, 2712–2720.
33 Y. Luo, Z. Teng and Q. Wang, Development of zein nanoparticles coated with carboxymethyl chitosan for encapsulation and controlled release of vitamin D3, *J. Agric. Food Chem.*, 2012, **60**, 836–843.
34 N. K. Deepak Chitkara, BSA-PLGA-Based Core-Shell Nanoparticles as Carrier System for Water-Soluble Drugs, *Pharm. Res.*, 2013, **30**, 2396–2409.
35 J. Ge, P. Yue, J. Chi, J. Liang and X. Gao, Formation and stability of anthocyanins-loaded nanocomplexes prepared with chitosan hydrochloride and carboxymethyl chitosan, *Food Hydrocolloids*, 2018, **74**, 23–31.
36 Y.-W. Wu, S.-Q. Sun, J. Zhao, Y. Li and Q. Zhou, Rapid discrimination of extracts of Chinese propolis and poplar buds by FT-IR and 2D IR correlation spectroscopy, *J. Mol. Struct.*, 2008, **883.-884**, 48–54.
37 V. B. de Souza, M. Thomazini, M. A. E. Barrientos, C. M. Nalin, R. Ferro-Furtado, M. I. Genovese and C. S. Favaro-Trindade, Functional properties and encapsulation of a proanthocyanidin-rich cinnamon extract (Cinnamomum zeylanicum) by complex coacervation using gelatin and different polysaccharides, *Food Hydrocolloids*, 2017, **77**, 297–306.
38 C. Chang, T. Wang, Q. Hu, M. Zhou, J. Xue and Y. Luo, Pectin coating improves physicochemical properties of caseinate/zein nanoparticles as oral delivery vehicles for curcumin, *Food Hydrocolloids*, 2017, **70**, 143–151.
39 F. O. M. S. Abreu, C. Bianchini, M. M. C. Forte and T. B. L. Kist, Influence of the composition and preparation method on the morphology and swelling behavior of alginate–chitosan hydrogels, *Carbohydr. Polym.*, 2008, **74**, 283–289.
40 L. Mao, W. Wang, K. Tai, F. Yuan and Y. Gao, Development of a soy protein isolate-carrageenan-quercetagetin noncovalent complex for the stabilization of beta-carotene emulsions, *Food Funct.*, 2017, **8**, 4356–4363.
41 J. K. Yan, W. Y. Qiu, Y. Y. Wang and J. Y. Wu, Biocompatible Polyelectrolyte Complex Nanoparticles from Lactoferrin and Pectin as Potential Vehicles for Antioxidative Curcumin, *J. Agric. Food Chem.*, 2017, **65**, 5720–5730.
42 A. Patel, E. C. Bouwens and K. P. Velikov, Sodium caseinate stabilized zein colloidal particles, *J. Agric. Food Chem.*, 2010, **58**, 12497–12503.
43 O. G. Jones, U. Lesmes, P. Dubin and D. J. McClements, Effect of polysaccharide charge on formation and properties of biopolymer nanoparticles created by heat treatment of β-lactoglobulin–pectin complexes, *Food Hydrocolloids*, 2010, **24**, 374–383.
44 B. Hu, M. Xie, C. Zhang and X. Zeng, Genipin-structured peptide-polysaccharide nanoparticles with significantly improved resistance to harsh gastrointestinal environments and their potential for oral delivery of polyphenols, *J. Agric. Food Chem.*, 2014, **62**, 12443–12452.
45 S. Moser, M. Chegeni, O. G. Jones, A. Liceaga and M. G. Ferruzzi, The effect of milk proteins on the bioaccessibility of green tea flavan-3-ols, *Food Res. Int.*, 2014, **66**, 297–305.